White matter disruption at the prodromal stage of Alzheimer's disease: Relationships with hippocampal atrophy and episodic memory performance

Florence Rémy [a,b,*], Nathalie Vayssière [a,b], Laure Saint-Aubert [c], Emmanuel Barbeau [a,b], Jérémie Pariente [d]

[a] Centre de Recherche Cerveau et Cognition, Université de Toulouse, UPS, France
[b] CNRS, CerCo, Toulouse, France
[c] Centre for Alzheimer Research, Department of Neurobiology, Division of Translational Alzheimer Neurobiology, Care Sciences and Society, Karolinska Institute, Stockholm, Sweden
[d] INSERM, Imagerie Cérébrale et Handicaps Neurologiques, Centre Hospitalier Universitaire de Toulouse, UMR 825, France

ARTICLE INFO

ABSTRACT

White matter tract alterations have been consistently described in Alzheimer's disease (AD). In particular, limbic fronto-temporal connections, which are critical to episodic memory function, may degenerate early in the course of the disease. However the relation between white matter tract degeneration, hippocampal atrophy and episodic memory impairment at the earliest stages of AD is still unclear. In this magnetic resonance imaging study, white matter integrity and hippocampal volumes were evaluated in patients with amnestic mild cognitive impairment due to AD (Albert et al., 2011) ($n = 22$) and healthy controls ($n = 15$). Performance in various episodic memory tasks was also evaluated in each participant. Relative to controls, patients showed a significant reduction of white matter fractional anisotropy (FA) and increase of radial diffusivity (RD) in the bilateral uncinate fasciculus, parahippocampal cingulum and fornix. Within the patient group, significant intra-hemispheric correlations were notably found between hippocampal grey matter volume and FA in the uncinate fasciculus, suggesting a relationship between atrophy and disconnection of the hippocampus. Moreover, episodic recognition scores were related with uncinate fasciculus FA across patients. These results indicate that fronto-hippocampal connectivity is reduced from the earliest pre-demential stages of AD. Disruption of fronto-hippocampal connections may occur progressively, in parallel with hippocampal atrophy, and may specifically contribute to early initial impairment in episodic memory.

1. Introduction

In vivo detection of the earliest physiological changes that occur in Alzheimer's disease (AD) is currently the focus of a large body of research. To identify the earliest cerebral biomarkers, imaging results are reported in patients with amnestic mild cognitive impairment (aMCI). These patients present with progressive episodic memory deficit and have a high risk to convert to AD dementia (Petersen et al., 1999). In aMCI patients relative to age-matched controls, significant medial temporal grey matter (GM) atrophy and hypometabolism at rest have been consistently reported (De Santi et al., 2001; Du et al., 2004; Jack et al., 1999; Pengas et al., 2010), coherent with the earliest neurofibrillary tangle deposition in the hippocampus and entorhinal cortex in AD (Braak and Braak, 1991). Besides, reduced metabolism has been reported in posterior cerebral regions, most consistently in the posterior cingulate cortex (PCC), in early AD (Chételat et al., 2003) and aMCI patients (Herholz et al., 2002; Minoshima et al., 1997; Nestor et al., 2003). Accordingly, several authors proposed that these functional changes may result from reduced connectivity of posterior regions with the hippocampus (Chételat et al., 2008, 2003; Minoshima et al., 1997; Nestor et al., 2003; Smith, 2002). Hippocampal disconnection may occur from very early stages of the disease, thus affecting large-scale neural networks critical to episodic memory, such as the limbic network (Callen et al., 2001; Huang et al., 2012; Nestor et al., 2003; Pengas et al., 2010). On the basis of this disconnection hypothesis (Chételat et al., 2003; Smith, 2002), an interesting approach is to evaluate potential changes in white matter (WM) tracts from the earliest stages of AD. The present study aimed at measuring WM changes in aMCI patients, who responded to strict physiological criteria typical of AD pathology, i.e. patients with aMCI due to AD (Albert et al., 2011; Dubois et al., 2014). Our objective was to identify the earliest alterations in WM connections that could contribute to the initial episodic memory impairment.

* Corresponding author at: Centre de Recherche Cerveau et Cognition, UMR 5549, CNRS UPS, Pavillon Baudot, CHU Purpan, 31059 Toulouse cedex 9, France. Tel.: +33 5 62 74 61 54.
E-mail address: florence.remy@cerco.ups-tlse.fr (F. Rémy).

Using magnetic resonance diffusion tensor imaging (MR-DTI) (Basser and Jones, 2002; Le Bihan et al., 2001), WM microstructural changes in aMCI patients have been most consistently reported in temporal and parietal regions (for review see Chua et al., 2008; Sexton et al., 2011), although frontal and occipital WM may also undergo changes (Bosch et al., 2012; Zhuang et al., 2010). These WM alterations could be more important as pathology evolves, as suggested in studies comparing aMCI and mild AD patients with controls (Bosch et al., 2012; Fellgiebel et al., 2005; Kiuchi et al., 2009; Liu et al., 2011; Medina et al., 2006; Mielke et al., 2009; Zhang et al., 2007). In particular, limbic WM tracts may be altered in aMCI, and further in AD patients. To date, the most consistent finding has been a significant alteration of the cingulum (Acosta-Cabronero et al., 2012; Bosch et al., 2012; Fellgiebel et al., 2005; Kiuchi et al., 2009; Liu et al., 2011; Medina et al., 2006; Rose et al., 2006; Stenset et al., 2011; Zhang et al., 2007; Zhuang et al., 2013), which connects the hippocampal formation with the cingulate gyrus (Catani and Thiebaut de Schotten, 2008). In AD patients, hippocampal volume has been related with alteration of the cingulum micro-structure (Choo et al., 2010; Xie et al., 2005), as well as with cingulum bundle volume (Villain et al., 2008), suggesting a causal link between the hippocampus and cingulum anatomical changes. Also, alteration of the cingulum is consistent with early PCC hypometabolism at rest (Chételat et al., 2003; Minoshima et al., 1997), and may in particular explain the relationship between hippocampal atrophy and PCC/temporo-parietal hypometabolism, which has been reported in AD (Meguro et al., 2001; Villain et al., 2008) and aMCI (Guedj et al., 2009) patients. Apart from the cingulum, other limbic tracts may as well undergo changes in early AD. Alterations of the fornix have been reported in aMCI patients (Mielke et al., 2009; Zhuang et al., 2013, 2010), and these alterations may be more important in patients with short-term progression to AD (Douaud et al., 2013). Also, damage of the uncinate fasciculus has been recently reported in 'late' aMCI (Zhuang et al., 2013) and more consistently in mild AD patients (Bosch et al., 2012; Damoiseaux et al., 2009; Kiuchi et al., 2009), this limbic tract connecting the temporal pole with the lower medial and lateral inferior frontal cortices (Catani and Thiebaut de Schotten, 2008). Notably, causal links were established between hippocampal GM atrophy, cingulum and uncinate fasciculus WM atrophy, and hypometabolism in the cingulate gyrus and lower frontal cortex (Villain et al., 2010). Together with the fornix, the cingulum and uncinate fasciculus are temporo-frontal limbic connections that underlie episodic memory function in healthy subjects (Metzler-Baddeley et al., 2011; Sepulcre et al., 2008). These WM tracts may get altered from the earliest prodromal stage of AD, leading to hippocampal disconnection with posterior and anterior cortical regions.

To date, the link between limbic WM damage and episodic memory impairment remains unclear. Whole-brain WM DTI metrics in aMCI patients have been previously related with cognitive status (Acosta-Cabronero et al., 2012; Mielke et al., 2009; Nir et al., 2013) and memory scores (Bosch et al., 2012; Fellgiebel et al., 2005). Note that most of the latter correlations were obtained across groups of subjects, pooling aMCI and AD patients (and sometimes controls), and this may artificially increase the correlation strength. Besides, episodic recall performance in aMCI patients has been related to DTI metrics in pre-defined regions of interest of the retrosplenial (Walhovd et al., 2009) and temporal WM (Goldstein et al., 2009), regions that could comprise the posterior and parahippocampal parts of the cingulum, respectively. However, clear relationships between damage of specific WM tracts and early episodic memory deficit in aMCI patients remain to be established. In particular, episodic *recognition* and *recall* of verbal/visual materials, which are both impaired early in AD, could rely on separate neural networks involving distinct hippocampal tracts. Whereas episodic recognition of previously-encoded items could be mostly based on item familiarity and involve hippocampal connections with anterior temporal and frontal regions (Gour et al., 2011), episodic recall may additionally recruit posterior regions, such as the PCC and temporo-parietal cortex (Wang et al., 2010), thus involving the cingulum tract.

In the present study, DTI-derived parameters in whole-brain WM tracts were measured in patients with aMCI due to AD (Albert et al., 2011; Dubois et al., 2014), and in age-matched controls. By selecting patients according to strict inclusion criteria, we expected to measure group differences specifically related to the earliest stages of AD pathology. It was previously reported that hippocampal connectivity with distant posterior and anterior brain regions could be reduced in early AD, as a consequence of hippocampal atrophy (Villain et al., 2010). We aimed at supporting this hypothesis using whole-brain WM DTI and hippocampal GM volumetry. Differences in WM micro-structure between patients and controls were assessed, and fibre tractography was computed from medial temporal regions showing significant changes, allowing for clear identification of altered tracts in patients. Correlations between hippocampal volumes and DTI metrics were then assessed in these regions. Moreover, performance in episodic recognition and recall of verbal and visual items was assessed in each participant. We hypothesized that initial impairment in episodic memory tasks may rely on early hippocampal disconnection, from the pre-demential stage of AD. Disruption of tracts connecting the hippocampus with anterior regions may mainly affect item recognition, whereas episodic recall deficit could be related with alterations of hippocampal tracts projecting to posterior regions.

2. Materials & methods

2.1. Participants

Twenty-two patients diagnosed with aMCI due to AD (see inclusion criteria below) and 15 age- and gender-matched control subjects were recruited for the study (Table 1). The study was approved by the regional Ethics committee (Comité de Protection des Personnes Sud-Ouest et Outre-Mer I, no. AFSSAPS A90605-58) and written informed consent was given by all participants.

2.2. Inclusion criteria

2.2.1. Patients with MCI due to AD

Pre-inclusion assessment and inclusion criteria have been extensively described in a previous report (Saint-Aubert et al., 2013). Briefly, patients over 65 years old, with a memory complaint dating from more than 6 months and without any neurologic or psychiatric disease history, were initially recruited ($n = 34$). After pre-inclusion assessment, which included neuropsychological tests (Clinical Dementia Rating (CDR) scale and Free and Cued Selective Reminding Test (FCSRT)), MRI examination, ^{18}F-FDG Positron Emission Tomography (PET) examination and cerebrospinal fluid (CSF) biomarker sampling, inclusion was decided according to the following criteria:

- CDR = 0.5, i.e. autonomy in daily life,
- Sum of the three free recalls ≤17/48 and/or sum of the three free and cued recalls ≤40/48 on the FCSRT, i.e. significant verbal episodic memory impairment (Sarazin et al., 2007),
- One or more of the following criteria:
  ◦ Scheltens score for medial temporal GM atrophy >1 in at least one hemisphere, based on visual T_1-weighted MRI scan examination (Scheltens et al., 1992).
  ◦ Temporo-parietal and/or PCC hypometabolism at rest suggestive of AD, based on visual FDG-PET scan examination.
  ◦ Level of phospho-tau (P-tau) ≥60 pg/ml and Innotest Amyloid Tau Index (IATI) ≤ 0.8. In case of ambiguous profile, i.e. P-tau < 60 pg/ml or IATI > 0.8, the Aβ42/Aβ40 level ratio was calculated and a ratio <0.045 was considered compatible with AD diagnosis (Wiltfang et al., 2007).

Moreover, patients with significant white matter hyperintensities on the T2-weighted MRI scan (Fazekas and Schmidt (F&S) score > 2 (Fazekas et al., 2002)) were excluded.

Table 1
Sociodemographic and neuropsychological features of patients and healthy controls.

	aMCI due to AD	Controls	p
n	22	15	
Gender (M:F)	10:12	7:8	n.s.
Age at MRI (years)	72.1 ± 4.9 (65–81)	70.5 ± 4.7 (65–80)	n.s.
Education (years)	11.6 ± 2.8 (8–17)	12.2 ± 3.0 (9–17)	n.s.
Disease duration (years)	3.8 ± 3.6 (1–11)		
CDR	0.5 ± 0.0	0.0 ± 0.0	<0.001
MMSE (/30)	25.0 ± 2.1 (20–28)	28.4 ± 0.7 (27–29)	<0.001
Verbal episodic memory — FCSRT			
Immediate recall (/16)	12.9 ± 2.8 (7–16)	15.5 ± 0.7 (14–16)	<0.001
Sum of the 3 free recalls (/48)	10.9 ± 6.3 (1–27)	32.1 ± 4.8 (24–39)	<0.001
Sum of the 3 free and cued recalls (/48)	27.3 ± 12.3 (7–47)	46.5 ± 2.0 (42–48)	<0.001
Sum of the 3 recognitions (/48)	43.7 ± 3.7 (34–48)	47.7 ± 0.8 (45–48)	<0.001
Delayed free recall (/16)	3.7 ± 3.0 (0–10)	12.7 ± 2.2 (9–16)	<0.001
Delayed free and cued recall (/16)	9.9 ± 5.2 (0–16)	15.7 ± 0.6 (14–16)	<0.001
Visual episodic memory — DMS48			
Immediate recognition (/48)	40.4 ± 5.7 (29–47)	46.3 ± 2.1 (41–48)	<0.001
Delayed recognition (/48)	39.3 ± 7.1 (24–48)	45.7 ± 2.2 (41–48)	<0.001
Visuo-spatial episodic memory			
Rey complex figure recall (/36)	8.3 ± 5.8 (0–20)	19.8 ± 6.4 (9–30)	<0.001
Composite memory scores			
Episodic recognition score	0.0 ± 0.83 (−1.59–1.11)		
Episodic recall score	0.0 ± 0.85 (−1.38–1.5)		

Values are mean ± standard deviation (range). CDR = Clinical Dementia Rating; MMSE = Mini-Mental State Examination; FCSRT = Free and Cued Selective Reminding Test; DMS48 = Delayed Matched Sample test. Composite memory scores were calculated in patients only.

Based on the above criteria, 22 patients out of 34 were included in the study. Among these included patients, 12 patients had positive CSF biomarker and positive degeneration biomarkers (both medial temporal GM atrophy and temporo-parietal/PCC hypometabolism) and 6 patients had positive CSF biomarker and one positive degeneration biomarker (2 with medial temporal GM atrophy and 4 with temporo-parietal/PCC hypometabolism). From the remaining 4 patients, 2 did not consent for CSF sampling: they had both medial temporal GM atrophy and temporo-parietal/PCC hypometabolism. One patient had negative CSF biomarker and 2 positive degeneration biomarkers. Finally, one patient had ambiguous CSF profile and 2 positive degeneration biomarkers.

Following their inclusion in the study, patients ($n = 22$) underwent a second PET scan using Florbetapir (AV-45) amyloid marker, as part of the imaging protocol (Saint-Aubert et al., 2013). Global AV-45 uptake in the GM was visually rated. Eighteen patients out of 22 had a positive cerebral Aβ biomarker, including the 2 patients without any CSF sampling and the patient with negative CSF biomarker. Thus combining results of CSF sampling and AV-45 PET imaging at the time of the study, 21 patients had at least one amyloid marker typical of AD pathology (with at least one positive degeneration marker), increasing confidence for diagnosis of aMCI due to AD (Albert et al., 2011; Dubois et al., 2014). The remaining patient showed low AV-45 uptake and ambiguous CSF profile. Following the study, all patients were evaluated every 6 months over a period of 2 years, as part of their clinical follow-up. During this 2-year period, 17 out of the 22 patients included in the study met the NIA–AA diagnostic criteria for dementia due to AD (McKhann et al., 2011). Note that the patient with ambiguous amyloid profile at the time of the study has been diagnosed with dementia due to AD during the 2-year follow-up.

2.2.2. Control subjects

Control subjects ($n = 25$) without any memory complaint, any neurologic or psychiatric disease history and any first-degree relative with AD, underwent identical pre-inclusion assessment as the patients (except for CSF sampling). Subjects with significant white matter hyperintensities on the T2-weighted MRI scan (F&S score > 2) or any impairment on the neuropsychological assessment were excluded. Following assessment, 15 control subjects satisfied inclusion criteria and completed their participation in the study. Three out of the 15 controls had not any positive degeneration biomarker, 9 controls had temporo-

parietal/PCC hypometabolism, 1 control had medial temporal GM atrophy and 2 controls had both atrophy and hypometabolism. Following cerebral Aβ assessment using AV-45 PET imaging, 4 control subjects were positively rated, with all of them also showing hypometabolism.

2.3. Neuropsychological assessment

To complement the pre-inclusion neuropsychological assessment, global cognitive state was evaluated using the Mini-Mental State Examination (MMSE) (Folstein et al., 1975). Furthermore, visuo-spatial episodic memory was assessed with delayed recall of the Rey–Osterrieth Complex Figure Test (RCFT) (Strauss et al., 2006). The Delayed Matched Sample (DMS48) test (Barbeau et al., 2004) was used to evaluate immediate and delayed visual object recognition. Other cognitive functions were also assessed, such as semantic memory, verbal working memory, language and attention. Details on these assessments have been previously reported (Saint-Aubert et al., 2013).

For the purpose of correlations with DTI metrics, two composite episodic memory scores were generated in each patient. A first composite *recognition* score was computed as the mean of 3 standardized scores: the sum of the 3 recognitions in the FCSRT, the immediate recognition and the delayed recognition in the DMS48. A second composite *recall* score was computed as the mean of 6 standardized scores: the immediate recall, the sum of the 3 free recalls, the sum of the 3 free and cued recalls, the delayed free recall, the delayed free and cued recall in the FCSRT, and the Rey figure recall.

2.4. MR imaging protocol

Scanning was performed on a Philips 3 T system (Achieva, Philips, Best, The Netherlands), using a dedicated 8-channel phased-array headcoil. T1-weighted and DTI images were acquired in a single scanning session for each participant.

Diffusion-weighted imaging was performed using a spin-echo single-shot echo-planar imaging sequence, with TR/TE = 11,031/55 ms, number of excitations (NEX) = 1 and an isotropic voxel size of $2 \times 2 \times 2$ mm. Fifty-six contiguous axial slices were positioned to cover the whole brain. Images were acquired for 32 non-collinear directions of the diffusion gradients (with $b = 1000$ s/mm^2, using a Philips default diffusion vector scheme) and one image was acquired with no diffusion weighting ($b = 0$, *b0* image), allowing for computation of

the diffusion tensor. Parallel acquisition (SENSE factor = 1.5) and partial k-space sampling (factor = 0.68) were used. The total scanning time was 7′33″.

In addition, a high-resolution high-contrast anatomical T1-weighted scan was acquired for hippocampal GM volumetry purposes. A 3D TFE gradient-echo sequence was used, with TR/TE = 8.3/3.8 ms, NEX = 1 and an isotropic voxel size of $1 \times 1 \times 1$ mm. One hundred and sixty coronal slices were acquired, covering the whole brain.

2.5. Hippocampal GM volumetry

The procedure for hippocampal GM volumetry has been previously described in detail (Cherubini et al., 2010). Briefly, individual T1-weighted images were segmented using the FIRST tool in FSL and volumes of the left and right hippocampi were determined by voxel count from the GM images. Hippocampal volumes were then corrected for individual whole-brain size. To this aim, volumes for each subject were multiplied by a scaling factor, which was determined based on the whole-brain volume expansion or contraction needed to register the individual T1-weighted image to the MNI template (Cherubini et al., 2010). The resulting normalized volumes were compared between groups using two-factor ANOVA (with between-subject 'group' factor and within-subject 'hemisphere' factor), and were further used to correlate DTI parameters with hippocampal atrophy (see below).

2.6. Diffusion imaging analysis

All analyses were performed using the Functional MRI of the Brain (FMRIB) software library (FSL v5.0.2.1, http://www.fmrib.ox.ac.uk/fsl) (Smith et al., 2004). For each participant, the 32 diffusion-weighted images were all re-aligned (using affine registration) to the *b0* image, in order to correct for eddy current distortion and head movements. A brain mask was created from the *b0* image ('BET' procedure in FSL) and the mask was applied to all images to remove non-brain tissue. Fitting of the diffusion tensor model in each voxel was performed using the DTIFIT procedure. Images of fractional anisotropy (FA), mean diffusivity (MD), axial diffusivity (AxD) and radial diffusivity (RD) were then derived from eigenvalues of the diffusion tensor, in each participant.

2.6.1. Patients with aMCI due to AD vs. controls

DTI-derived variables were compared between groups with a whole-brain approach, using the tract-based spatial statistics (TBSS v1.2) method (Smith et al., 2006). Following slight erosion, FA images of each subject were all non-linearly registered to a 1-mm isotropic FA standard-space image ('FMRIB58_FA') (Rueckert et al., 1999). The resulting FA images from all participants were then averaged, and a mean white-matter tract skeleton was calculated from the mean FA image (threshold at 0.2). This skeleton represents the centre of major tracts that would be common to all subjects. For every participant, the nearest tract centre (as determined from the individual spatially-normalized FA image) was projected onto the mean FA skeleton. Voxel-wise statistics were computed using permutation-based (non parametric) tests, as implemented in the 'randomize' program of FSL. All tests were performed with 5000 random permutations of the data. In all analyses, a cluster-based approach was used with the threshold-free cluster enhancement (TFCE) procedure (Smith and Nichols, 2009). Two-sample unpaired *t*-tests were used to compare DTI-derived variables between patients and controls, covarying out the effect of age, sex and years of education. Clusters significant at $p < 0.05$, family-wise error (FWE) corrected, are reported. In clusters of interest, i.e. most probably belonging to limbic hippocampo-frontal connections, average FA and diffusivity values were calculated for every subject, and effect sizes were derived (with 95% confidence interval). Moreover, these clusters of interest were back-projected to the centre of the nearest tract on the individual FA images in standard space, in order to ensure that the skeleton cluster was

derived from the correct tract-centre points in all subjects (Smith et al., 2006). Finally, for each control subject, WM tracts passing through these clusters were determined individually. To this aim, clusters were transformed back to the subject's native space using an inverse non-linear registration to the one originally applied for the subject. These clusters in native space were then used as seed masks for probabilistic tractography using the FSL algorithm 'probtrackx', after Bayesian estimation of diffusion parameters from the individual realigned diffusion images ('bedpostx' function in FSL) (Behrens et al., 2007).

2.6.2. Correlations with hippocampal volumes and memory scores across patients

In the patient group ($n = 22$), correlations between average DTI-derived variables in clusters of interest (as determined from the group comparison analysis, see above) and (i) normalized left and right hippocampal GM volumes, and (ii) composite episodic memory scores were assessed in a linear regression model, including age, MMSE, sex and years of education as nuisance covariates. Significant correlations within the patient group at a threshold of $p < 0.05$ (Bonferroni-corrected for the number of comparisons) are reported, along with determination coefficients (R squared).

In addition, whole-brain correlations between DTI variables and (i) hippocampal volumes, and (ii) composite memory scores were examined using TBSS. Positive and negative correlations were investigated. Age, MMSE, sex and years of educations were entered into the analyses as covariates. Clusters significant at $p < 0.05$ (FWE-corrected) using the TFCE procedure are reported.

3. Results

3.1. Neuropsychological data

In all aspects of episodic memory that were tested, i.e. verbal, visual and visuo-spatial, patients were significantly impaired relative to controls (Table 1). Across the patient sample, ranges of episodic memory scores were rather large, allowing for optimal investigation of correlations between WM DTI-metrics and performance. Regarding other cognitive functions, semantic memory (based on Wechsler Adult Intelligence Scale (WAIS) information subtest and TOP 12 faces scores) and executive functions (based on semantic verbal fluency, Trail Making Test (TMT), Symbol Digit Modalities Test and Stroop Test scores) were also significantly impaired in patients vs. controls (for more detailed results, see Saint-Aubert et al., 2013).

3.2. Hippocampal GM volumes

Total hippocampal volumes were significantly reduced in patients relative to controls ($p < 0.002$, Table 2). Moreover, hippocampal atrophy in patients was significant in both the left and right hemispheres ($p < 0.004$ and $p < 0.007$ respectively) and was equivalent for both hemispheres ($F(1,35) = 0.13$, $p = 0.72$, repeated-measures ANOVA). The large range of hippocampal volumes across patients allowed for optimal investigation of correlations between DTI-metrics and GM atrophy.

Table 2
Normalized hippocampal volumes (in mm³) for patients and healthy controls.

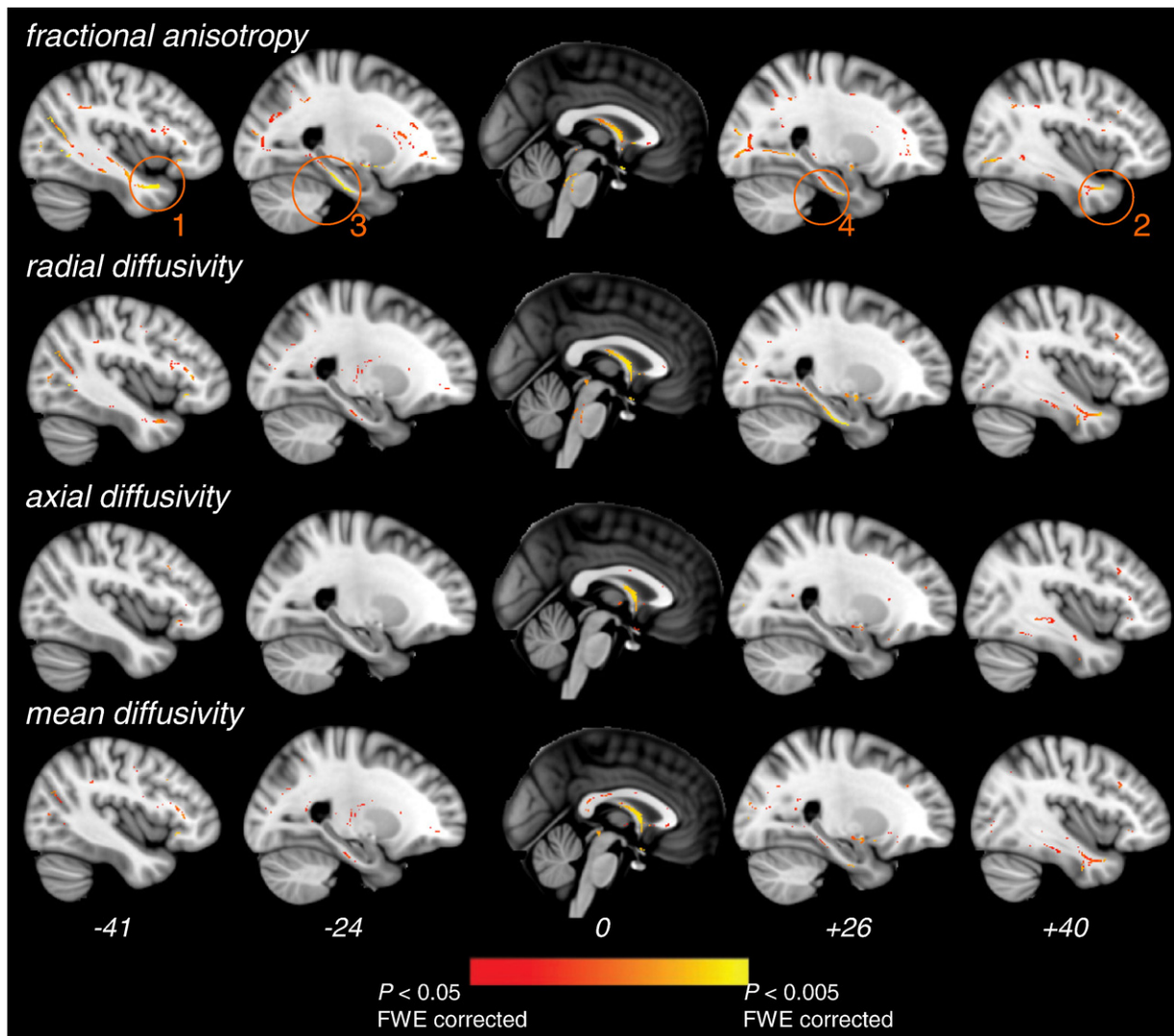|	aMCI due to AD	Controls	*p*
Right	6115 ± 905 (4217–7943)	6881 ± 711 (5644–7878)	0.007
Left	5821 ± 948 (4122–7298)	6676 ± 714 (5494–7910)	0.004
Total	11,936 ± 1682 (9116–15,156)	13,557 ± 1270 (11,184–15,705)	0.002

Values are mean ± standard deviation (range).

Fig. 1. Significant differences in DTI metrics between patients and controls. Regions of decreased fractional anisotropy and increased radial, axial and mean diffusivities in patients vs. controls are displayed. Medial temporal clusters showing significant FA decreases in patients are highlighted (orange circles). These clusters were further used as seed masks for tractography and as ROIs for correlation analyses within patients (see the Materials and methods section). All clusters shown are significant at $p < 0.05$ FWE-corrected for multiple comparisons using threshold-free cluster enhancement. DTI metrics and skeleton are superimposed on a standard T1 template. MNI x coordinates are indicated at the bottom of each slice.

3.3. Whole-brain DTI metrics

3.3.1. Patients vs. controls comparison

In patients vs. controls, the FA was reduced and the diffusivity indexes were increased in widespread WM regions (Fig. 1). Conversely, there was not any significant increase in FA or decrease in diffusivity in patients vs. controls ($p < 0.05$ corrected). Reduced FA values in patients relative to controls were found in WM tracts of the lateral temporal, parietal, frontal and occipital lobes, most probably corresponding to the anterior thalamic radiations, the temporal part of the superior longitudinal fasciculus bilaterally, the occipital and temporal parts of the inferior longitudinal fasciculus bilaterally, and the inferior fronto-occipital fasciculus bilaterally. Moreover, patients' FA was lower in the fornix (local peak at (0, 7, 2)), in the medial temporal region bilaterally (bilateral anterior temporal lobe: local peaks at (−41, 2, −27) and (40, 9, −30), respectively clusters 1 and 2 on Fig. 1, and hippocampal regions: local peaks at (−24, −12, −31) and (26, −8, −32), respectively clusters 3 and 4 on Fig. 1) and in the cortico-spinal tract (superior corona radiata and at the level of the brainstem). In highly similar WM regions, the RD and MD were greater in patients relative to controls (Fig. 1). A significant increase in MD was also found in the splenium and genu

of the corpus callosum. In patients vs. controls, increases in AxD were confined to the right temporal and frontal WM, and the fornix.

Since the 4 medial temporal clusters found in the group comparison analysis (clusters 1–4 on Fig. 1) were close to sites of cortical atrophy in early AD, i.e. the hippocampus and anterior parahippocampal gyrus, these medial temporal skeleton voxels were back-projected to the centre of the nearest WM tract in each individual FA image. Supplementary Fig. 1 displays the result of back-projection of skeleton voxels for each patient, showing that accurate WM points were considered in the group comparison analysis for each of the 4 clusters. Finally, fibre tractography was conducted in each of the control subjects using the 4 clusters as seed masks, in order to precisely determine WM tracts passing through these clusters. When taking the left and right anterior temporal clusters as seed masks (respectively clusters 1 and 2 on Fig. 1), left- and right-sided U-shaped tracts starting from the temporal pole and projecting to the inferior medial frontal cortex, i.e. the left and right uncinate fasciculi (Catani and Thiebaut de Schotten, 2008), were evidenced in each control (Supplementary Fig. 1). For the 2 other clusters in the left and right hippocampal regions (respectively clusters 3 and 4 on Fig. 1), tractography revealed 2 symmetrical medial tracts connecting the anterior part of the medial temporal lobe to the posterior

Table 3
DTI metrics in WM tracts of interest.

		aMCI due to AD	Controls	Effect size
Fractional anisotropy				
Uncinate fasciculus	L	0.264 ± 0.052	0.315 ± 0.044	−0.051 (−0.083, −0.019)
	R	0.229 ± 0.043	0.278 ± 0.045	−0.049 (−0.080, −0.019)
Parahippocampal cingulum	L	0.301 ± 0.026	0.340 ± 0.031	−0.039 (−0.058, −0.018)
	R	0.264 ± 0.042	0.299 ± 0.025	−0.035 (−0.057, −0.012)
Fornix		0.452 ± 0.080	0.520 ± 0.038	−0.068 (−0.108, −0.028)
Radial diffusivity				
Uncinate fasciculus	L	0.687 ± 0.070	0.633 ± 0.075	0.054 (0.004, 0.104)
	R	0.770 ± 0.100	0.715 ± 0.049	0.055 (0.005, 0.106)
Parahippocampal cingulum	L	0.683 ± 0.043	0.647 ± 0.049	0.036 (0.004, 0.068)
	R	0.712 ± 0.041	0.656 ± 0.040	0.056 (0.029, 0.083)
Fornix		0.997 ± 0.141	0.858 ± 0.130	0.139 (0.047, 0.230)
Axial diffusivity				
Fornix		2.046 ± 0.107	1.928 ± 0.111	0.118 (0.043, 0.193)
Mean diffusivity				
Uncinate fasciculus	R	0.899 ± 0.075	0.847 ± 0.051	0.052 (0.010, 0.094)
Parahippocampal cingulum	L	0.817 ± 0.042	0.785 ± 0.048	0.032 (0.001, 0.064)
	R	0.833 ± 0.048	0.796 ± 0.044	0.037 (0.006, 0.068)
Fornix		1.257 ± 0.157	1.099 ± 0.131	0.158 (0.061, 0.255)

Values are mean ± standard deviation. Effect sizes are difference in means between groups (95% confidence interval). Effect sizes are overestimated, as metrics were extracted from most significant voxels in the group comparison.

cingulate cortex, i.e. the parahippocampal part of the cingulum (Catani and Thiebaut de Schotten, 2008) (Supplementary Fig. 1).

In all limbic clusters found in the group comparison analysis (clusters 1–4 and fornix), average DTI metrics were computed in each subject and effect sizes were derived in each region (Table 3).

3.3.2. Correlations with hippocampal volume within the patient group

In each limbic cluster (clusters 1–4 and fornix), correlations between average DTI metrics and left and right hippocampal volumes (HVs) were investigated. Regarding diffusivity metrics, there was not any significant correlation with HV, in any of the clusters (corrected $p < 0.05$). However positive correlations were found between FA and HV (Fig. 2). In the fornix, the FA was significantly correlated with the right HV ($R^2 = 0.337$, corrected $p = 0.025$). The correlation between fornix FA and left HV was not significant ($p = 0.62$). In the right parahippocampal cingulum (cluster 4 on Fig. 1), the FA was correlated with the right HV ($R^2 = 0.307$, corrected $p = 0.04$) but not with the left HV ($p = 0.31$). In the left parahippocampal cingulum (cluster 3 on Fig. 1), the FA was correlated with the left HV ($R^2 = 0.431$, corrected $p = 0.005$) and with the right HV ($R^2 = 0.34$, corrected $p = 0.02$). Finally, the FA in the right uncinate fasciculus (cluster 2 on Fig. 1) was significantly correlated with the right HV ($R^2 = 0.33$, corrected $p = 0.03$) but not with the left HV ($p = 0.3$). Conversely, the FA in the left uncinate fasciculus (cluster 1 on Fig. 1) was correlated with the left HV ($R^2 = 0.376$, corrected $p = 0.015$) but not with the right HV ($p = 0.88$).

The whole-brain correlation analyses on FA values were consistent with the above ROI results in the limbic regions ($p < 0.05$ FWE-corrected, Fig. 2). Left HVs were correlated with predominantly left-sided temporal and parietal FA measures. In particular, significant correlations with the left anterior temporal FA (local peak at (−41, 9, −29)) and the left hippocampal FA (local peak at (−24, −31, −17)) were found. Besides, right HVs were correlated with FA values in the corpus callosum, and the lateral occipital, parietal, temporal and right frontal regions. Regarding limbic regions, FA measures in

the right anterior temporal region (local peak at (40, 0, −28)), the bilateral hippocampal region (right hemisphere: local peak at (26, −34, −12); left hemisphere: local peak at (−20, −37, −10), not shown on Fig. 2) and the fornix (local peak at (4, −20, 18)) were correlated with volumes of the right hippocampus. Other whole-brain analyses on diffusivity measures did not show any significant correlations with HVs.

3.3.3. Correlations with episodic performance within the patient group

In each limbic cluster (clusters 1–4 and fornix), correlations between average DTI metrics and composite episodic memory scores (Table 1) were investigated. There was not any significant correlation between diffusivity metrics and composite memory scores, in any of the limbic clusters (corrected $p < 0.05$). Regarding the FA metric, only one significant positive correlation with composite recognition scores was found in the left uncinate fasciculus (cluster 1 on Fig. 1, $R^2 = 0.359$, corrected $p = 0.022$, Fig. 3). Other correlations between FA in limbic tracts and composite recognition and recall scores did not reach significance (corrected $p > 0.2$).

Whole-brain TBSS analyses did not evidence any significant correlation between diffusivity measures and memory scores ($p < 0.05$ FWE-corrected). The correlation between FA and composite recognition scores was significant in the left anterior temporal region (local peak at (−38, 6, −32), Fig. 3), in agreement with the above ROI result. There was not any significant correlation between FA and composite recall scores ($p < 0.05$ FWE-corrected).

4. Discussion

In the present study, WM tract integrity was evaluated in patients with aMCI due to AD (Albert et al., 2011; Dubois et al., 2014) and age-matched controls, using MRI diffusion tensor imaging. Our results clearly evidenced disease-related WM changes in limbic tracts, suggesting disruption of hippocampal connections with remote cortical regions early in the course of AD. These WM changes were related with patients' performance in some aspects of episodic memory, showing that hippocampal disconnection may partly explain initial memory impairment at the pre-demential stage of the disease.

In patients relative to controls, the FA was reduced and the RD was increased in limbic and long association tracts. Widespread changes in DTI metrics have been consistently reported in bilateral limbic and association tracts at different stages of the disease, from presymptomatic (Molinuevo et al., 2014) to aMCI (Acosta-Cabronero et al., 2012; Bosch et al., 2012) and mild AD stages (Acosta-Cabronero et al., 2010). At the prodromal stage, axonal loss and demyelination (Bartzokis, 2004) would contribute to reduce the FA and increase the RD within WM tracts, as a result of enlarged extra-cellular diffusion space between axonal membranes (Beaulieu, 2006). Conversely, recent studies in presymptomatic AD patients have reported either increases in FA together with decreases in diffusivity relative to controls (Racine et al., 2014; Ryan et al., 2013) or no changes in FA but increases in AxD (Molinuevo et al., 2014). It was proposed that pathological changes such as swelling of neurons, microgliosis or amyloid deposits may underlie changes in DTI metrics before symptom onset (Racine et al., 2014; Ryan et al., 2013). In our study, there was not any WM region showing increased FA and/or reduced diffusivity in patients. This indicates that changes in DTI metrics critically depend on disease stage and most probably on selection criteria for patients, underlining the need for full exploration of the tensor behaviour in AD studies (Acosta-Cabronero et al., 2010). Regarding the prodromal stage of AD, our results suggest that FA changes may capture the result of ongoing neurodegenerative process better than other DTI metrics. The FA may therefore be the most pertinent parameter to investigate WM alterations in relation with initial cognitive decline (Acosta-Cabronero et al., 2012).

Our imaging data evidenced WM tract alterations in the limbic system, in patients relative to controls. These alterations were found in
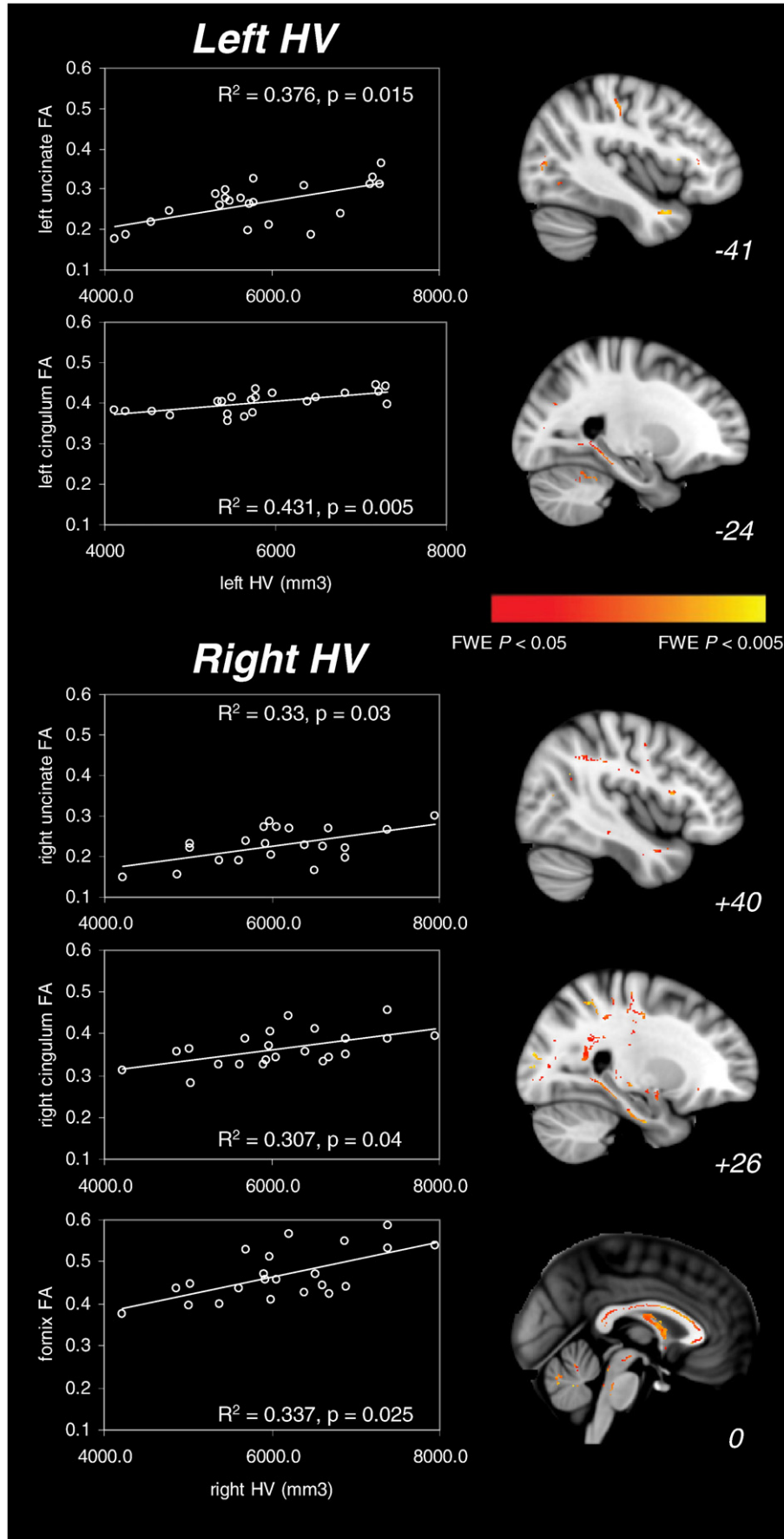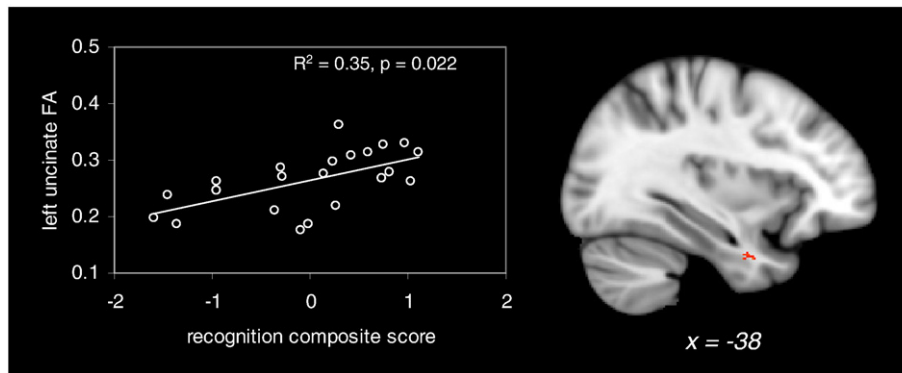
Fig. 3. Significant correlation between composite episodic recognition score and left uncinate fasciculus FA in the patient group (*p* < 0.05 Bonferroni-corrected for multiple comparisons). The right side of the figure shows the result of the whole-brain correlation between FA values and composite recognition scores. Significant clusters are superimposed on a standard T1 template. MNI *x* coordinate is indicated at the bottom of the sagittal slice.

the parahippocampal cingulum, the uncinate fasciculus and in the fornix, i.e. in fronto-temporal connections critical to episodic memory (Metzler-Baddeley et al., 2011). Moreover, FA values in these 3 limbic tracts were found to correlate with hippocampal volume across patients. In agreement, correlations between GM volume and cingulum FA have been previously reported in AD patients (Firbank et al., 2007; Xie et al., 2005) or combining aMCI and AD patients (Choo et al., 2010). Using voxel-based morphometry in aMCI patients, the atrophy rate of the cingulum and uncinate fasciculus (measured over an 18-month period) was found to correlate with baseline hippocampal GM atrophy (Villain et al., 2010). The authors proposed that disruption of both these limbic tracts, occurring in early AD, may be a consequence of neuronal loss in the hippocampus. Our correlation results in pre-demential AD patients fully support this hypothesis. In our study, the correlation between uncinate fasciculus FA and hippocampal GM volume was observed separately within each hemisphere. Intra-hemispheric correlations support the idea that axonal loss due to Wallerian degeneration may be the primary cause of FA decreases in these limbic tracts, although this causal link needs to be further confirmed using a longitudinal design (Villain et al., 2010). The temporal segment of the uncinate fasciculus connects the entorhinal and perirhinal cortices with the temporal pole (Von Der Heide et al., 2013), and the entorhinal cortex is the very first site of neuronal death in AD (Braak and Braak, 1991). Therefore damage in the uncinate fasciculus could be tightly related with anterior medial temporal GM atrophy (Damoiseaux et al., 2009; Villain et al., 2010) and could begin from the earliest stages of the disease. Regarding the cingulum, its parahippocampal part connects the hippocampus with the PCC (Vann et al., 2009). The FA decrease and RD increase in this tract may be a consequence of hippocampal neuronal loss, as previously proposed (Choo et al., 2010; Villain et al., 2010). Hypometabolism at rest in the PCC has been consistently shown in aMCI patients (Ewers et al., 2011). Moreover, PCC activity during episodic memory tasks has been correlated with hippocampal GM volume (Garrido et al., 2002; Rémy et al., 2005). De-afferentation of the PCC (Chetelat et al., 2003; Smith, 2002) may therefore contribute to its dysfunction from the aMCI stage (Minoshima et al., 1997; Nestor et al., 2003; Villain et al., 2010). It should be noted however that GM atrophy in this latter region has been observed in aMCI (Choo et al., 2010) and incipient AD (Pengas et al., 2010), suggesting that PCC hypometabolism could also partly result from local pathology.

Although the strength of hippocampal connections with other limbic structures cannot be simply derived from our anatomical data (Jones et al., 2013), it is important to note that our results are coherent with functional connectivity studies in AD (Allen et al., 2007; Bai et al., 2009; Greicius et al., 2004; Sorg et al., 2009; Wang et al., 2007). Using resting-state functional MRI, these studies have shown decreased hippocampal functional connectivity with the PCC and the lower medial prefrontal cortex. Therefore damage in the cingulum and uncinate fasciculus could contribute to altered hippocampal functional connectivity with posterior and anterior medial areas of the default-mode network in AD patients. Rate of decline of cingulate and inferior frontal glucose metabolism (measured over an 18-month period) was shown to correlate with cingulum and uncinate WM atrophy, respectively (Villain et al., 2010). This suggests that hypometabolism in limbic regions would be a consequence of damage in hippocampal connections. Specific alteration of the cingulum and uncinate tracts in pre-demential AD is clearly confirmed in our study, using a different methodological approach assessing WM micro-structure. Moreover, it has been observed that aMCI patients show distinctive patterns of metabolic decrease according to clinical outcome (Fouquet et al., 2009). Whereas all patients showed metabolic decreases in the PCC and medial frontal cortex, AD converters evidenced specific metabolic decreases in the ventral prefrontal cortex, most probably resulting from disconnection between medial temporal and lower frontal regions. This result clearly argues in favour of an alteration of the uncinate fasciculus at the prodromal stage of AD, in total agreement with our findings. In further support, anterior temporal WM atrophy, most probably corresponding to the temporal part of the uncinate fasciculus, was found in aMCI patients who converted to AD within an average of 15 months, relative to non-converters (ADNI study (Misra et al., 2009)). This underlines again the specificity of this tract disruption at an early stage of the pathology.

Significant correlations between uncinate fasciculus FA values and composite episodic recognition scores across patients were observed in our study. These composite scores were representative of immediate and delayed recognition performance of verbal or visual materials. In the monkey, temporo-prefrontal disconnection by section of the uncinate fasciculus leads to impairment in delayed matching-to-sample tasks (Gaffan and Wilson, 2008). In humans, FA in the uncinate fasciculus has been correlated with performance in associative visual object–location memory (Metzler-Baddeley et al., 2011; Von Der Heide et al., 2013). The uncinate fasciculus is part of an 'anterior temporal network',

Fig. 2. Significant positive correlations between hippocampal volumes (HV) and FA measures in the patient group. The left part of the figure displays significant correlations between FA values in limbic tracts of interest and left and right hippocampal volumes. *p*-Values are Bonferroni-corrected for multiple comparisons. The right part of the figure shows whole-brain correlations between FA values and left HV (upper part) and right HV (bottom part) as a result of the TBSS analysis (*p* < 0.05 FWE-corrected). Significant clusters are superimposed on a standard T1 template. MNI *x* coordinates are indicated at the bottom of each sagittal plane.

as previously described (Gour et al., 2011; Kahn et al., 2008). This network, which includes the anterior hippocampus and sub-hippocampal structures, the lateral temporal cortex and the temporal pole, and which receives input from the visual ventral stream, could be involved in familiarity-based recognition of single items (Gour et al., 2011). Consistently, we found that performance in recognition of verbal and visual items, which may strongly rely on familiarity-based processing, was related with uncinate fasciculus integrity in our group of patients. Besides, it should be noted that the uncinate fasciculus has been given a role in social and emotional processing of stimuli (Von Der Heide et al., 2013) and its role in the emergence of mood disorders in early AD has been proposed (Fouquet et al., 2009). Our correlation analysis did not evidence any link between FA in limbic tracts and episodic recall deficit across patients. Episodic recall may rely on both direct and indirect fronto-temporal connections, due to the use of specific memory strategies, thus involving both anterior and posterior networks (Kahn et al., 2008). Therefore alteration in the uncinate and cingulum tracts, as well as in the fornix (Metzler-Baddeley et al., 2011), together would contribute to impairment in recall. This latter hypothesis would not be captured using whole-brain single correlation analysis between recall scores and FA, as performed in our study.

In summary, our results support the hypothesis that limbic tracts connecting temporal and frontal lobes are likely disrupted from the earliest stage of AD. This degeneration seems to be closely related with, and possibly a consequence of, medial temporal GM atrophy (Villain et al., 2010). In addition to cingulum micro-structure alteration largely reported in aMCI, we found progressive alteration of the uncinate fasciculus in prodromal AD patients, further supporting previous observations in demented patients. Degeneration of the uncinate fasciculus may impact episodic recognition performance very early in the disease.

Supplementary data to this article can be found online at http://dx.doi.org/10.1016/j.nicl.2015.01.014.

References

Acosta-Cabronero, J., Alley, S., Williams, G.B., Pengas, G., Nestor, P.J., 2012. Diffusion tensor metrics as biomarkers in Alzheimer's disease. PLOS One 7 (11), e49072. http://dx.doi.org/10.1371/journal.pone.0049072.

Acosta-Cabronero, J., Williams, G.B., Pengas, G., Nestor, P.J., 2010. Absolute diffusivities define the landscape of white matter degeneration in Alzheimer's disease. Brain 133 (2), 529–539. http://dx.doi.org/10.1093/brain/awp25719914928.

Albert, M.S., DeKosky, S.T., Dickson, D., Dubois, B., Feldman, H.H., Fox, N.C., Gamst, A., Holtzman, D.M., Jagust, W.J., Petersen, R.C., Snyder, P.J., Carrillo, M.C., Thies, B., Phelps, C.H., 2011. The diagnosis of mild cognitive impairment due to Alzheimer's disease: recommendations from the National Institute on Aging–Alzheimer's Association workgroups on diagnostic guidelines for Alzheimer's disease. Alzheimers Dement. 7 (3), 270–279. http://dx.doi.org/10.1016/j.jalz.2011.03.008.

Allen, G., Barnard, H., McColl, R., Hester, A.L., Fields, J.A., Weiner, M.F., Ringe, W.K., Lipton, A.M., Brooker, M., McDonald, E., Rubin, C.D., Cullum, C.M., 2007. Reduced hippocampal functional connectivity in Alzheimer disease. Arch. Neurol. 64 (10), 1482–1487. http://dx.doi.org/10.1001/archneur.64.10.148217923631.

Bai, F., Zhang, Z., Watson, D.R., Yu, H., Shi, Y., Yuan, Y., Zang, Y., Zhu, C., Qian, Y., 2009. Abnormal functional connectivity of hippocampus during episodic memory retrieval processing network in amnestic mild cognitive impairment. Biol. Psychiatry 65 (11), 951–958. http://dx.doi.org/10.1016/j.biopsych.2008.10.01719028382.

Barbeau, E., Didic, M., Tramoni, E., Felician, O., Joubert, S., Sontheimer, A., Ceccaldi, M., Poncet, M., 2004. Evaluation of visual recognition memory in MCI patients. Neurology 62 (8), 1317–1322. http://dx.doi.org/10.1212/01.WNL.0000120548.24298.DB15111668.

Bartzokis, G., 2004. Age-related myelin breakdown: a developmental model of cognitive decline and Alzheimer's disease. Neurobiol. Aging 25 (1), 5–18. http://dx.doi.org/10.1016/j.neurobiolaging.2003.03.00114675724.

Basser, P.J., Jones, D.K., 2002. Diffusion-tensor MRI: theory, experimental design and data analysis — a technical review. NMR Biomed. 15 (7–8), 456–467. http://dx.doi.org/10.1002/nbm.78312489095.

Beaulieu, C., 2006. Biophysical underpinnings of diffusion. ISMRM Educational Session Annual Meeting 1–6.

Behrens, T.E., Berg, H.J., Jbabdi, S., Rushworth, M.F., Woolrich, M.W., 2007. Probabilistic diffusion tractography with multiple fibre orientations: what can we gain? Neuroimage 34 (1), 144–155. http://dx.doi.org/10.1016/j.neuroimage.2006.09.01817070705.

Bosch, B., Arenaza-Urquijo, E.M., Rami, L., Sala-Llonch, R., Junqué, C., Solé-Padullés, C., Peña-Gómez, C., Bargalló, N., Molinuevo, J.L., Bartrés-Faz, D., 2012. Multiple DTI index analysis in normal aging, amnestic MCI and AD. Relationship with neuropsychological performance. Neurobiol. Aging 33 (1), 61–74. http://dx.doi.org/10.1016/j.neurobiolaging.2010.02.00420371138.

Braak, H., Braak, E., 1991. Neuropathological staging of Alzheimer-related changes. Acta Neuropathol. 82 (4), 239–259. http://dx.doi.org/10.1007/BF003088091759558.

Callen, D.J., Black, S.E., Gao, F., Caldwell, C.B., Szalai, J.P., 2001. Beyond the hippocampus: MRI volumetry confirms widespread limbic atrophy in AD. Neurology 57 (9), 1669–1674. http://dx.doi.org/10.1212/WNL.57.9.166911706109.

Catani, M., Thiebaut de Schotten, M., 2008. A diffusion tensor tractography atlas for virtual in vivo dissections. Cortex 44 (8), 1105–1132. http://dx.doi.org/10.1016/j.cortex.2008.05.00418619589.

Cherubini, A., Péran, P., Spoletini, I., Di Paola, M., Di Iulio, F., Hagberg, G.E., Sancesario, G., Gianni, W., Bossù, P., Caltagirone, C., Sabatini, U., Spalletta, G., 2010. Combined volumetry and DTI in subcortical structures of mild cognitive impairment and Alzheimer's disease patients. J. Alzheimers Dis. 19 (4), 1273–1282. http://dx.doi.org/10.3233/JAD-2010-09118620308792.

Chételat, G., Desgranges, B., de la Sayette, V., Viader, F., Berkouk, K., Landeau, B., Lalevée, C., Le Doze, F., Dupuy, B., Hannequin, D., Baron, J.-C., Eustache, F., 2003b. Dissociating atrophy and hypometabolism impact on episodic memory in mild cognitive impairment. Brain 126 (9), 1955–1967. http://dx.doi.org/10.1093/brain/awg19612821520.

Chételat, G., Desgranges, B., Landeau, B., Mézenge, F., Poline, J.B., de la Sayette, V., Viader, F., Eustache, F., Baron, J.-C., 2008. Direct voxel-based comparison between grey matter hypometabolism and atrophy in Alzheimer's disease. Brain 131 (1), 60–71. http://dx.doi.org/10.1093/brain/awm28818063588.

Choo, I.H., Lee, D.Y., Oh, J.S., Lee, J.S., Lee, D.S., Song, I.C., Youn, J.C., Kim, S.G., Kim, K.W., Jhoo, J.H., Woo, J.I., 2010. Posterior cingulate cortex atrophy and regional cingulum disruption in mild cognitive impairment and Alzheimer's disease. Neurobiol. Aging 31 (5), 772–779. http://dx.doi.org/10.1016/j.neurobiolaging.2008.06.01518687503.

Chua, T.C., Wen, W., Slavin, M.J., Sachdev, P.S., 2008. Diffusion tensor imaging in mild cognitive impairment and Alzheimer's disease: a review. Curr. Opin. Neurol. 21 (1), 83–92. http://dx.doi.org/10.1097/WCO.0b013e3282f4594b18180656.

Damoiseaux, J.S., Smith, S.M., Witter, M.P., Sanz-Arigita, E.J., Barkhof, F., Scheltens, P., Stam, C.J., Zarei, M., Rombouts, S.A., 2009. White matter tract integrity in aging and Alzheimer's disease. Hum. Brain Mapp. 30 (4), 1051–1059. http://dx.doi.org/10.1002/hbm.2056318412132.

De Santi, S., De Leon, M.J., Rusinek, H., Convit, A., Tarshish, C.Y., Roche, A., Tsui, W.H., Kandil, E., Boppana, M., Daisley, K., Wang, G.J., Schlyer, D., Fowler, J., 2001. Hippocampal formation glucose metabolism and volume losses in MCI and AD. Neurobiol. Aging 22 (4), 529–539. http://dx.doi.org/10.1016/S0197-4580(01)00230-511445252.

Douaud, G., Menke, R.A., Gass, A., Monsch, A.U., Rao, A., Whitcher, B., Zamboni, G., Matthews, P.M., Sollberger, M., Smith, S., 2013. Brain microstructure reveals early abnormalities more than two years prior to clinical progression from mild cognitive impairment to Alzheimer's disease. J. Neurosci. 33 (5), 2147–2155. http://dx.doi.org/10.1523/JNEUROSCI.4437-12.201323365250.

Du, A.T., Schuff, N., Kramer, J.H., Ganzer, S., Zhu, X.P., Jagust, W.J., Miller, B.L., Reed, B.R., Mungas, D., Yaffe, K., Chui, H.C., Weiner, M.W., 2004. Higher atrophy rate of entorhinal cortex than hippocampus in AD. Neurology 62 (3), 422–427. http://dx.doi.org/10.1212/01.WNL.0000106462.72282.9014872024.

Dubois, B., Feldman, H.H., Jacova, C., Hampel, H., Molinuevo, J.L., Blennow, K., DeKosky, S.T., Gauthier, S., Selkoe, D., Bateman, R., Cappa, S., Crutch, S., Engelborghs, S., Frisoni, G.B., Fox, N.C., Galasko, D., Habert, M.-O., Jicha, G.A., Nordberg, A., Pasquier, F., Rabinovici, G., Robert, P., Rowe, C., Salloway, S., Sarazin, M., Epelbaum, S., de Souza, L.C., Vellas, B., Visser, P.J., Schneider, L., Stern, Y., Scheltens, P., Cummings, J.L., 2014. Advancing research diagnostic criteria for Alzheimer's disease: the IWG-2 criteria. Lancet Neurol. 13 (6), 614–629. http://dx.doi.org/10.1016/S1474-4422(14)70090-024849862.

Ewers, M., Sperling, R.A., Klunk, W.E., Weiner, M.W., Hampel, H., 2011. Neuroimaging markers for the prediction and early diagnosis of Alzheimer's disease dementia. Trends Neurosci. 34 (8), 430–442. http://dx.doi.org/10.1016/j.tins.2011.05.00521996658.

Fazekas, F., Barkhof, F., Wahlund, L.O., Pantoni, L., Erkinjuntti, T., Scheltens, P., Schmidt, R., 2002. CT and MRI rating of white matter lesions. Cerebrovasc. Dis. 13 (Suppl. 2), 31–36 49147] [Pubmed: 11901240].

Fellgiebel, A., Müller, M.J., Wille, P., Dellani, P.R., Scheurich, A., Schmidt, L.G., Stoeter, P., 2005. Color-coded diffusion-tensor-imaging of posterior cingulate fiber tracts in mild cognitive impairment. Neurobiol. Aging 26 (8), 1193–1198. http://dx.doi.org/10.1016/j.neurobiolaging.2004.11.00615917103.

Firbank, M.J., Blamire, A.M., Krishnan, M.S., Teodorczuk, A., English, P., Gholkar, A., Harrison, R., O'Brien, J.T., 2007. Atrophy is associated with posterior cingulate white matter disruption in dementia with Lewy bodies and Alzheimer's disease. Neuroimage 36 (1), 1–7. http://dx.doi.org/10.1016/j.neuroimage.2007.02.02717142610.

Folstein, M.F., Folstein, S.E., McHugh, P.R., 1975. "Mini-mental state". A practical method for grading the cognitive state of patients for the clinician. J. Psychiatr. Res. 12 (3), 189–198. http://dx.doi.org/10.1016/0022-3956(75)90026-61202204.

Fouquet, M., Desgranges, B., Landeau, B., Duchesnay, E., Mézenge, F., de la Sayette, V., Viader, F., Baron, J.-C., Eustache, F., Chételat, G., 2009. Longitudinal brain metabolic

changes from amnestic mild cognitive impairment to Alzheimer's disease. Brain 132 (8), 2058–2067. http://dx.doi.org/10.1093/brain/awp13219477964.

Gaffan, D., Wilson, C.R., 2008. Medial temporal and prefrontal function: recent behavioural disconnection studies in the macaque monkey. Cortex 44 (8), 928–935. http://dx.doi.org/10.1016/j.cortex.2008.03.00518585697.

Garrido, G.E., Furuie, S.S., Buchpiguel, C.A., Bottino, C.M., Almeida, O.P., Cid, C.G., Camargo, C.H., Castro, C.C., Glabus, M.F., Busatto, G.F., 2002. Relation between medial temporal atrophy and functional brain activity during memory processing in Alzheimer's disease: a combined MRI and SPECT study. J. Neurol. Neurosurg. Psychiatry 73 (5), 508–516. http://dx.doi.org/10.1136/jnnp.73.5.50812397142.

Goldstein, F.C., Mao, H., Wang, L., Ni, C., Lah, J.J., Levey, A.I., 2009. White matter integrity and episodic memory performance in mild cognitive impairment: a diffusion tensor imaging study. Brain Imaging Behav. 3 (2), 132–141. http://dx.doi.org/10.1007/s11682-008-9055-y20596297.

Gour, N., Ranjeva, J.-P., Ceccaldi, M., Confort-Gouny, S., Barbeau, E., Soulier, E., Guye, M., Didic, M., Felician, O., 2011. Basal functional connectivity within the anterior temporal network is associated with performance on declarative memory tasks. Neuroimage 58 (2), 687–697. http://dx.doi.org/10.1016/j.neuroimage.2011.05.09021722740.

Greicius, M.D., Srivastava, G., Reiss, A.L., Menon, V., 2004. Default-mode network activity distinguishes Alzheimer's disease from healthy aging: evidence from functional MRI. Proc. Natl. Acad. Sci. U. S. A. 101 (13), 4637–4642. http://dx.doi.org/10.1073/pnas.030862710115070770.

Guedj, E., Barbeau, E.J., Didic, M., Felician, O., de Laforte, C., Ranjeva, J.-P., Poncet, M., Cozzone, P.J., Mundler, O., Ceccaldi, M., 2009. Effects of medial temporal lobe degeneration on brain perfusion in amnestic MCI of AD type: deafferentation and functional compensation? Eur. J. Nucl. Med. Mol. Imaging 36 (7), 1101–1112. http://dx.doi.org/10.1007/s00259-009-1060-x19224210.

Herholz, K., Salmon, E., Perani, D., Baron, J.C., Holthoff, V., Frölich, L., Schönknecht, P., Ito, K., Mielke, R., Kalbe, E., Zündorf, G., Delbeuck, X., Pelati, O., Anchisi, D., Fazio, F., Kerrouche, N., Desgranges, B., Eustache, F., Beuthien-Baumann, B., Menzel, C., Schröder, J., Kato, T., Arahata, Y., Henze, M., Heiss, W.D., 2002. Discrimination between Alzheimer dementia and controls by automated analysis of multicenter FDG PET. Neuroimage 17 (1), 302–316. http://dx.doi.org/10.1006/nimg.2002.120812482085.

Huang, H., Fan, X., Weiner, M., Martin-Cook, K., Xiao, G., Davis, J., Devous, M., Rosenberg, R., Diaz-Arrastia, R., 2012. Distinctive disruption patterns of white matter tracts in Alzheimer's disease with full diffusion tensor characterization. Neurobiol. Aging 33 (9), 2029–2045. http://dx.doi.org/10.1016/j.neurobiolaging.2011.06.02721872362.

Jack, C.R., Petersen, R.C., Xu, Y.C., O'Brien, P.C., Smith, G.E., Ivnik, R.J., Boeve, B.F., Waring, S.C., Tangalos, E.G., Kokmen, E., 1999. Prediction of AD with MRI-based hippocampal volume in mild cognitive impairment. Neurology 52 (7), 1397–1403. http://dx.doi.org/10.1212/WNL.52.7.139710227624.

Jones, D.K., Knösche, T.R., Turner, R., 2013. White matter integrity, fiber count, and other fallacies: the do's and don'ts of diffusion MRI. Neuroimage 73, 239–254. http://dx.doi.org/10.1016/j.neuroimage.2012.06.08122846632.

Kahn, I., Andrews-Hanna, J.R., Vincent, J.L., Snyder, A.Z., Buckner, R.L., 2008. Distinct cortical anatomy linked to subregions of the medial temporal lobe revealed by intrinsic functional connectivity. J. Neurophysiol. 100 (1), 129–139. http://dx.doi.org/10.1152/jn.00077.200818385483.

Kiuchi, K., Morikawa, M., Taoka, T., Nagashima, T., Yamauchi, T., Makinodan, M., Norimoto, K., Hashimoto, K., Kosaka, J., Inoue, Y., Inoue, M., Kichikawa, K., Kishimoto, T., 2009. Abnormalities of the uncinate fasciculus and posterior cingulate fasciculus in mild cognitive impairment and early Alzheimer's disease: a diffusion tensor tractography study. Brain Res. 1287, 184–191. http://dx.doi.org/10.1016/j.brainres.2009.06.05219559010.

Le Bihan, D., Mangin, J.F., Poupon, C., Clark, C.A., Pappata, S., Molko, N., Chabriat, H., 2001. Diffusion tensor imaging: concepts and applications. J. Magn. Reson. Imaging 13 (4), 534–546. http://dx.doi.org/10.1002/jmri.107611276097.

Liu, Y., Spulber, G., Lehtimäki, K.K., Könönen, M., Hallikainen, I., Gröhn, H., Kivipelto, M., Hallikainen, M., Vanninen, R., Soininen, H., 2011. Diffusion tensor imaging and tract-based spatial statistics in Alzheimer's disease and mild cognitive impairment. Neurobiol. Aging 32 (9), 1558–1571. http://dx.doi.org/10.1016/j.neurobiolaging.2009.10.00619913331.

McKhann, G.M., Knopman, D.S., Chertkow, H., Hyman, B.T., Jack, C.R., Kawas, C.H., Klunk, W.E., Koroshetz, W.J., Manly, J.J., Mayeux, R., Mohs, R.C., Morris, J.C., Rossor, M.N., Scheltens, P., Carrillo, M.C., Thies, B., Weintraub, S., Phelps, C.H., 2011. The diagnosis of dementia due to Alzheimer's disease: recommendations from the National Institute on Aging–Alzheimer's Association workgroups on diagnostic guidelines for Alzheimer's disease. Alzheimers Dement. 7 (3), 263–269. http://dx.doi.org/10.1016/j.jalz.2011.03.005.

Medina, D., DeToledo-Morrell, L., Urresta, F., Gabrieli, J.D., Moseley, M., Fleischman, D., Bennett, D.A., Leurgans, S., Turner, D.A., Stebbins, G.T., 2006. White matter changes in mild cognitive impairment and AD: a diffusion tensor imaging study. Neurobiol. Aging 27 (5), 663–672. http://dx.doi.org/10.1016/j.neurobiolaging.2005.03.02616005548.

Meguro, K., LeMestric, C., Landeau, B., Desgranges, B., Eustache, F., Baron, J.C., 2001. Relations between hypometabolism in the posterior association neocortex and hippocampal atrophy in Alzheimer's disease: a PET/MRI correlative study. J. Neurol. Neurosurg. Psychiatr. 71, 315–32111511703.

Metzler-Baddeley, C., Jones, D.K., Belaroussi, B., Aggleton, J.P., O'Sullivan, M.J., 2011. Frontotemporal connections in episodic memory and aging: a diffusion MRI tractography study. J. Neurosci. 31 (37), 13236–13245. http://dx.doi.org/10.1523/JNEUROSCI.2317-11.201121917806.

Mielke, M.M., Kozauer, N.A., Chan, K.C., George, M., Toroney, J., Zerrate, M., Bandeen-Roche, K., Wang, M.-C., Vanzijl, P., Pekar, J.J., Mori, S., Lyketsos, C.G., Albert, M., 2009. Regionally-specific diffusion tensor imaging in mild cognitive impairment

and Alzheimer's disease. Neuroimage 46 (1), 47–55. http://dx.doi.org/10.1016/j.neuroimage.2009.01.05419457371.

Minoshima, S., Giordani, B., Berent, S., Frey, K.A., Foster, N.L., Kuhl, D.E., 1997. Metabolic reduction in the posterior cingulate cortex in very early Alzheimer's disease. Ann. Neurol. 42 (1), 85–94. http://dx.doi.org/10.1002/ana.4104201149225689.

Misra, C., Fan, Y., Davatzikos, C., 2009. Baseline and longitudinal patterns of brain atrophy in MCI patients, and their use in prediction of short-term conversion to AD: results from ADNI. Neuroimage 44 (4), 1415–1422. http://dx.doi.org/10.1016/j.neuroimage.2008.10.03119027862.

Molinuevo, J.L., Ripolles, P., Simó, M., Lladó, A., Olives, J., Balasa, M., Antonell, A., Rodriguez-Fornells, A., Rami, L., 2014. White matter changes in preclinical Alzheimer's disease: a magnetic resonance imaging–diffusion tensor imaging study on cognitively normal older people with positive amyloid β protein 42 levels. Neurobiol. Aging 35, 2671–2680. http://dx.doi.org/10.1016/j.neurobiolaging.2014.05.02725002037.

Nestor, P.J., Fryer, T.D., Smielewski, P., Hodges, J.R., 2003. Limbic hypometabolism in Alzheimer's disease and mild cognitive impairment. Ann. Neurol. 54 (3), 343–351. http://dx.doi.org/10.1002/ana.1066912953266.

Nir, T.M., Jahanshad, N., Villalon-Reina, J.E., Toga, A.W., Jack, C.R., Weiner, M.W., Thompson, P.M., Alzheimer's Disease Neuroimaging Initiative (ADNI), 2013. Effectiveness of regional DTI measures in distinguishing Alzheimer's disease, MCI, and normal aging. Neuroimage Clin. 3, 180–195. http://dx.doi.org/10.1016/j.nicl.2013.07.00624179862.

Pengas, G., Hodges, J.R., Watson, P., Nestor, P.J., 2010. Focal posterior cingulate atrophy in incipient Alzheimer's disease. Neurobiol. Aging 31 (1), 25–33. http://dx.doi.org/10.1016/j.neurobiolaging.2008.03.01418455838.

Petersen, R.C., Smith, G.E., Waring, S.C., Ivnik, R.J., Tangalos, E.G., Kokmen, E., 1999. Mild cognitive impairment: clinical characterization and outcome. Arch. Neurol. 56 (3), 303–308. http://dx.doi.org/10.1001/archneur.56.3.30310190820.

Racine, A.M., Adluru, N., Alexander, A.L., Christian, B.T., Okonkwo, O.C., Oh, J., Cleary, C.A., Birdsill, A., Hillmer, A.T., Murali, D., Barnhart, T.E., Gallagher, C.L., Carlsson, C.M., Rowley, H.A., Dowling, N.M., Asthana, S., Sager, M.A., Bendlin, B.B., Johnson, S.C., 2014. Associations between white matter microstructure and amyloid burden in preclinical Alzheimer's disease: a multimodal imaging investigation. Neuroimage Clin. 4, 604–614. http://dx.doi.org/10.1016/j.nicl.2014.02.00124936411.

Rémy, F., Mirrashed, F., Campbell, B., Richter, W., 2005. Verbal episodic memory impairment in Alzheimer's disease: a combined structural and functional MRI study. Neuroimage 25 (1), 253–266. http://dx.doi.org/10.1016/j.neuroimage.2004.10.04515734360.

Rose, S.E., McMahon, K.L., Janke, A.L., O'Dowd, B., de Zubicaray, G., Strudwick, M.W., Chalk, J.B., 2006. Diffusion indices on magnetic resonance imaging and neuropsychological performance in amnestic mild cognitive impairment. J. Neurol. Neurosurg. Psychiatry 77 (10), 1122–1128. http://dx.doi.org/10.1136/jnnp.2005.07433616754694.

Rueckert, D., Sonoda, L.I., Hayes, C., Hill, D.L., Leach, M.O., Hawkes, D.J., 1999. Non-rigid registration using free-form deformations: application to breast MR images. IEEE Trans. Med. Imaging 18 (8), 712–721. http://dx.doi.org/10.1109/42.79628410534053.

Ryan, N.S., Keihaninejad, S., Shakespeare, T.J., Lehmann, M., Crutch, S.J., Malone, I.B., Thornton, J.S., Mancini, L., Hyare, H., Yousry, T., Ridgway, G.R., Zhang, H., Modat, M., Alexander, D.C., Rossor, M.N., Ourselin, S., Fox, N.C., 2013. Magnetic resonance imaging evidence for presymptomatic change in thalamus and caudate in familial Alzheimer's disease. Brain 136 (5), 1399–1414. http://dx.doi.org/10.1093/brain/awt06523539189.

Saint-Aubert, L., Barbeau, E.J., Péran, P., Nemmi, F., Vervueren, C., Mirabel, H., Payoux, P., Hitzel, A., Bonneville, F., Gramada, R., Tafani, M., Vincent, C., Puel, M., Dechaumont, S., Chollet, F., Pariente, J., 2013. Cortical florbetapir-PET amyloid load in prodromal Alzheimer's disease patients. EJNMMI Res. 3 (1), 43. http://dx.doi.org/10.1186/2191-219X-3-4323731789.

Sarazin, M., Berr, C., De Rotrou, J., Fabrigoule, C., Pasquier, F., Legrain, S., Michel, B., Puel, M., Volteau, M., Touchon, J., Verny, M., Dubois, B., 2007. Amnestic syndrome of the medial temporal type identifies prodromal AD: a longitudinal study. Neurology 69 (19), 1859–1867. http://dx.doi.org/10.1212/01.wnl.0000279336.36610.f717984454.

Scheltens, P., Leys, D., Barkhof, F., Huglo, D., Weinstein, H.C., Vermersch, P., Kuiper, M., Steinling, M., Wolters, E.C., Valk, J., 1992. Atrophy of medial temporal lobes on MRI in "probable" Alzheimer's disease and normal ageing: diagnostic value and neuropsychological correlates. J. Neurol. Neurosurg. Psychiatry 55 (10), 967–972. http://dx.doi.org/10.1136/jnnp.55.10.9671431963.

Sepulcre, J., Masdeu, J.C., Sastre-Garriga, J., Goñi, J., Vélez-de-Mendizábal, N., Duque, B., Pastor, M.A., Bejarano, B., Villoslada, P., 2008. Mapping the brain pathways of declarative verbal memory: evidence from white matter lesions in the living human brain. Neuroimage 42 (3), 1237–1243. http://dx.doi.org/10.1016/j.neuroimage.2008.05.03818585467.

Sexton, C.E., Kalu, U.G., Filippini, N., Mackay, C.E., Ebmeier, K.P., 2011. A meta-analysis of diffusion tensor imaging in mild cognitive impairment and Alzheimer's disease. Neurobiol. Aging 32 (2322), e5–18.

Smith, A.D., 2002. Imaging the progression of Alzheimer pathology through the brain. Proc. Natl. Acad. Sci. U. S. A. 99 (7), 4135–4137. http://dx.doi.org/10.1073/pnas.08210739911929987.

Smith, S.M., Jenkinson, M., Johansen-Berg, H., Rueckert, D., Nichols, T.E., Mackay, C.E., Watkins, K.E., Ciccarelli, O., Cader, M.Z., Matthews, P.M., Behrens, T.E., 2006. Tract-based spatial statistics: voxelwise analysis of multi-subject diffusion data. Neuroimage 31 (4), 1487–1505. http://dx.doi.org/10.1016/j.neuroimage.2006.02.02416624579.

Smith, S.M., Jenkinson, M., Woolrich, M.W., Beckmann, C.F., Behrens, T.E., Johansen-Berg, H., Bannister, P.R., De Luca, M., Drobnjak, I., Flitney, D.E., Niazy, R.K., Saunders, J.,

Vickers, J., Zhang, Y., De Stefano, N., Brady, J.M., Matthews, P.M., 2004. Advances in functional and structural MR image analysis and implementation as FSL. Neuroimage 23 (Suppl. 1), S208–S219. http://dx.doi.org/10.1016/j.neuroimage.2004.07.05115501092.

Smith, S.M., Nichols, T.E., 2009. Threshold-free cluster enhancement: addressing problems of smoothing, threshold dependence and localisation in cluster inference. Neuroimage 44 (1), 83–98. http://dx.doi.org/10.1016/j.neuroimage.2008.03.06118501637.

Sorg, C., Riedl, V., Perneczky, R., Kurz, A., Wohlschläger, A.M., 2009. Impact of Alzheimer's disease on the functional connectivity of spontaneous brain activity. Curr. Alzheimer Res. 6 (6), 541–553. http://dx.doi.org/10.2174/15672050979014170619747154.

Stenset, V., Bjørnerud, A., Fjell, A.M., Walhovd, K.B., Hofoss, D., Due-Tønnessen, P., Gjerstad, L., Fladby, T., 2011. Cingulum fiber diffusivity and CSF T-tau in patients with subjective and mild cognitive impairment. Neurobiol. Aging 32 (4), 581–589. http://dx.doi.org/10.1016/j.neurobiolaging.2009.04.01419428143.

Strauss, E.H., Sherman, E.M.S., Spreen, O.. A, 2006. Compendium of Neuropsychological Tests: Administration, Norms, and Commentary. Oxford University Press, USA.

Vann, S.D., Aggleton, J.P., Maguire, E.A., 2009. What does the retrosplenial cortex do? Nat. Rev. Neurosci. 10 (11), 792–802. http://dx.doi.org/10.1038/nrn273319812579.

Villain, N., Desgranges, B., Viader, F., de la Sayette, V., Mézenge, F., Landeau, B., Baron, J.-C., Eustache, F., Chételat, G., 2008. Relationships between hippocampal atrophy, white matter disruption, and gray matter hypometabolism in Alzheimer's disease. J. Neurosci. 28 (24), 6174–6181. http://dx.doi.org/10.1523/JNEUROSCI.1392-08.200818550759.

Villain, N., Fouquet, M., Baron, J.-C., Mézenge, F., Landeau, B., de la Sayette, V., Viader, F., Eustache, F., Desgranges, B., Chételat, G., 2010. Sequential relationships between grey matter and white matter atrophy and brain metabolic abnormalities in early Alzheimer's disease. Brain 133 (11), 3301–3314. http://dx.doi.org/10.1093/brain/awq20320688814.

Von Der Heide, R.J., Skipper, L.M., Klobusicky, E., Olson, I.R., 2013. Dissecting the uncinate fasciculus: disorders, controversies and a hypothesis. Brain 136 (6), 1692–1707. http://dx.doi.org/10.1093/brain/awt09423649697.

Walhovd, K.B., Fjell, A.M., Amlien, I., Grambaite, R., Stenset, V., Bjørnerud, A., Reinvang, I., Gjerstad, L., Cappelen, T., Due-Tønnessen, P., Fladby, T., 2009. Multimodal imaging in mild cognitive impairment: metabolism, morphometry and diffusion of the tempo-ral–parietal memory network. Neuroimage 45 (1), 215–223. http://dx.doi.org/10.1016/j.neuroimage.2008.10.05319056499.

Wang, K., Liang, M., Wang, L., Tian, L., Zhang, X., Li, K., Jiang, T., 2007. Altered functional connectivity in early Alzheimer's disease: a resting-state fMRI study. Hum. Brain Mapp. 28 (10), 967–978. http://dx.doi.org/10.1002/hbm.2032417133390.

Wang, L., Laviolette, P., O'Keefe, K., Putcha, D., Bakkour, A., Van Dijk, K.R., Pihlajamäki, M., Dickerson, B.C., Sperling, R.A., 2010. Intrinsic connectivity between the hippocampus and posteromedial cortex predicts memory performance in cognitively intact older individuals. Neuroimage 51 (2), 910–917. http://dx.doi.org/10.1016/j.neuroimage.2010.02.04620188183.

Wiltfang, J., Esselmann, H., Bibl, M., Hüll, M., Hampel, H., Kessler, H., Frölich, L., Schröder, J., Peters, O., Jessen, F., Luckhaus, C., Perneczky, R., Jahn, H., Fiszer, M., Maler, J.M., Zimmermann, R., Bruckmoser, R., Kornhuber, J., Lewczuk, P., 2007. Amyloid beta peptide ratio 42/40 but not A beta 42 correlates with phospho-Tau in patients with low- and high-CSF A beta 40 load. J. Neurochem. 101 (4), 1053–1059. http://dx.doi.org/10.1111/j.1471-4159.2006.04404.x17254013.

Xie, S., Xiao, J.X., Wang, Y.H., Wu, H.K., Gong, G.L., Jiang, X.X., 2005. Evaluation of bilateral cingulum with tractography in patients with Alzheimer's disease. Neuroreport 16 (12), 1275–1278. http://dx.doi.org/10.1097/01.wnr.0000174061.41897.ee16056124.

Zhang, Y., Schuff, N., Jahng, G.-H., Bayne, W., Mori, S., Schad, L., Mueller, S., Du, A.-T., Kramer, J.H., Yaffe, K., Chui, H., Jagust, W.J., Miller, B.L., Weiner, M.W., 2007. Diffusion tensor imaging of cingulum fibers in mild cognitive impairment and Alzheimer disease. Neurology 68 (1), 13–19. http://dx.doi.org/10.1212/01.wnl.0000250326.77323.0117200485.

Zhuang, L., Sachdev, P.S., Trollor, J.N., Reppermund, S., Kochan, N.A., Brodaty, H., Wen, W., 2013. Microstructural white matter changes, not hippocampal atrophy, detect early amnestic mild cognitive impairment. PLOS One 8 (3), e58887. http://dx.doi.org/10.1371/journal.pone.005888723516569.

Zhuang, L., Wen, W., Zhu, W., Trollor, J., Kochan, N., Crawford, J., Reppermund, S., Brodaty, H., Sachdev, P., 2010. White matter integrity in mild cognitive impairment: a tract-based spatial statistics study. Neuroimage 53 (1), 16–25. http://dx.doi.org/10.1016/j.neuroimage.2010.05.06820595067.